Fast dynamic analysis of damaged 1D periodic waveguides

Alvaro Gavilán Rojas, Qinghua Zhang, Olivier Robin, Christophe Droz

Available online at www.sciencedirect.com

ScienceDirect

IFAC PapersOnline CONFERENCE PAPER ARCHIVE

IFAC PapersOnLine 58-15 (2024) 325–329

Fast dynamic analysis of damaged 1D periodic waveguides

Alvaro Gavilán Rojas [*,**] **Qinghua Zhang** [*] **Olivier Robin** [**] **Christophe Droz** [*]

[*] *Univ. Gustave Eiffel, Inria, I4S team, Rennes, France (e-mails: {alvaro.gavilan-rojas, qinghua.zhang, christophe.droz}@inria.fr).*
[**] *Centre de Recherche Acoustique-Signal-Humain, Université de Sherbrooke, Canada (e-mail: olivier.robin@usherbrooke.ca)*

Abstract: We extend the Bloch wave-based reduced order models in the Wave Finite Element Method (WFEM) framework for fast wave-damage interaction analysis. It aims at fault detection and diagnosis of periodic structures. A finned tube heat exchanger, which can be seen as a 1D system, is used as a numerical application. Reduced model results and performance are compared to a standard WFEM model. Diffusion curves are obtained more than a hundred times faster with the proposed scheme, moving toward massive generation of wave-damage scenarios and indicators to perform damage detection.

Keywords: Fault detection, model reduction, guided waves, periodic waveguides, Bloch waves.

1. INTRODUCTION

Ultrasonic guided waves are already part of current non-destructive evaluation practice, and they are becoming increasingly popular in the structural health monitoring field, its industrial deployment and standardization being well established for energy and transport industries such as oil and gas pipes, as well as rails (Cawley (2018); Ricci et al. (2022)). Damages like cracks or corrosion in such one dimensional waveguides induce reflections of injected elastic waves (compressional, torsional or flexural modes), and resulting reflections allow a long-range (~ 50 m) inspection of the structure, possibly identifying (i.e., locating and quantifying) these structural defects.

This paper is focused on the damage identification problem in periodic structures, i.e., a structure composed of repetitive geometrical forms or unit cells. Typical examples of such structures are airframes, sandwich panels, architectured materials or a finned tube heat exchanger, which is the presented model for numerical validation. Wave propagation is relatively simple in homogeneous structures like tubes, cylinders and plates, but it is much more complicated in these periodic structures where bandgaps, mode conversion and multiple reflections take place. It is thus important to develop suitable methods for the wave-damage interaction analysis to successfully identify damages in periodic structures. This could be greatly helped by numerical simulations and machine learning techniques to perform data-driven and physics-based analysis (Willberg et al. (2015); Fiborek and Kudela (2021)) where several damage models would be used to assess the nondestructive evaluation method performance.

Among the many numerical methods to simulate wave propagation in periodic waveguides, the Wave Finite Element Method (WFEM), initially developed by Mead (1973), constitutes a numerically efficient way for dispersion, forced response and diffusion analysis, by reducing the problem of periodic waveguides to that of a single unit cell. Moreover, free wave modes that propagate in the waveguide (Bloch modes) can be used to describe its dynamic motion, in the same way as the modal decomposition for modal analysis. This wave mode decomposition or *Bloch wave expansion* is of standard use in the WFEM literature (Mencik and Ichchou (2005); Mead (2009)).

More importantly, computational cost reductions are obtained by means of a reduced order model (ROM), and among the published methods in the WFEM context, the Bloch wave ROM proposed in Boukadia et al. (2018); Droz et al. (2014) leads to significant computation time reduction factors when applied to dispersion curves and forced response analysis. This ROM strategy is extended here to the context of diffusion analysis, i.e., the wave-based model reduction of a coupling element to obtain reflection and transmission curves. Its results and performances are compared against the Bloch wave expansion method (standard WFEM).

Any remarkable time reduction in the wave-damage interaction analysis would encourage the exploration of massively generated wave-damage scenarios (damage identification performance) and indicators (frequency responses, scattering coefficients) to assess the structural integrity by means of machine learning techniques, with vast amounts of labeled guided waves and damages. This could open the way to multiple scattering problems, complex damage models using non-linear approaches, and more generally the development of digital twins.

In this paper, we develop an efficient diffusion formulation based on the Bloch wave ROM that yields a well determined reduced linear system, providing us faster dynamic analysis results that could generate a database of wave-damage scenarios.

10.1016/j.ifacol.2024.08.549

2. WAVE FINITE ELEMENT METHOD (WFEM) FRAMEWORK

The Wave Finite Element Method (Mead (1973); Duhamel et al. (2006)), begin with a numerical finite element (FE)-discretized model description of the unit cell of a periodic waveguide, involving its mass, damping and stiffness matrices $\mathbf{M}$, $\mathbf{C}$, and $\mathbf{K}$, all being real symmetric and of size n_d, which is equal to the number of degrees of freedom of the unit cell. The size of the unit cell is d, that represents the distance between its left and right boundaries, which have the same mesh in order to numerically assemble the unit cells forming a waveguide.

In harmonic regime, the equation of motion of a unit cell is written $\mathbb{D}\mathbf{q} = \mathbf{f}$, where $\mathbf{q} \in \mathbb{C}^{n_d}$ are the nodal displacements, $\mathbf{f} \in \mathbb{C}^{n_d}$ the nodal forces, and $\mathbb{D} = -\omega^2\mathbf{M} + j\omega\mathbf{C} + \mathbf{K}$ is the *dynamic stiffness matrix*, with $\omega \in \mathbb{R}$ the angular frequency. We separate all the degrees of freedom of a unit cell into three parts, L and R for those at left and right boundaries and I for the inner ones. Accordingly, $\mathbb{D}, \mathbf{q}$ and $\mathbf{f}$ are partitioned and indexed by L, R and I. Considering that external loads will be applied only at the side boundaries of the unit cell, i.e., $\mathbf{f}_I = \mathbf{0}$ for the internal nodes, we can write the *condensed equation of motion*:

$$\begin{bmatrix} \mathbf{D}_{LL} & \mathbf{D}_{LR} \\ \mathbf{D}_{RL} & \mathbf{D}_{RR} \end{bmatrix} \begin{Bmatrix} \mathbf{q}_L \\ \mathbf{q}_R \end{Bmatrix} = \begin{Bmatrix} \mathbf{f}_L \\ \mathbf{f}_R \end{Bmatrix} \tag{1}$$

where $\mathbf{D}_{jk} = \mathbb{D}_{jk} - \mathbb{D}_{jI}\mathbb{D}_{II}^{-1}\mathbb{D}_{Ik} \quad \forall j, k \in \{L,\ R\}$.

An infinite waveguide can be assembled from the unit cell, as depicted in Figure 1. Free wave propagation is found when $\mathbf{q}_R = \lambda\mathbf{q}_L$ and $\mathbf{f}_R = -\lambda\mathbf{f}_L$, with $\lambda = \exp(ikd)$ being the *propagation constant*, $k \in \mathbb{C}$ the wavenumber. The complex displacement and force vectors at the interfaces are of size n, the number of degrees of freedom at the left and right boundaries. The internal force equilibrium at each of the interfaces of an assembled infinite waveguide gives us the following quadratic eigenvalue problem:

$$(\lambda^2\mathbf{D}_{LR} + \lambda(\mathbf{D}_{LL} + \mathbf{D}_{RR}) + \mathbf{D}_{RL})\boldsymbol{\phi} = \mathbf{0} \tag{2}$$

The $2n$ eigenvalues λ are the propagation constants, and the $2n$ eigenvectors $\boldsymbol{\phi} \in \mathbb{C}^n$ are the nodal displacements at a side boundary from which the Bloch waves (wave modes of free wave propagation in periodic media) can be recovered.

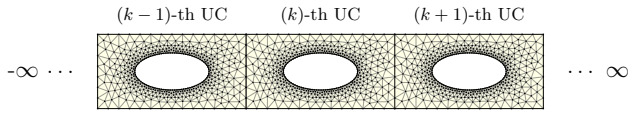

Fig. 1. Infinite 1D periodic waveguide.

Partial eigensolutions of (2) can be obtained to form a Bloch wave basis, consisting of those for which $|\lambda| \approx 1$. This is done with an iterative Arnoldi method on a linearized form of (2) proposed by Huang et al. (2009).

Considering a set of $2s$ solutions to form a partial Bloch basis, the s right-going are collected in $\boldsymbol{\Phi}^+$ and the s left-going wave modes in $\boldsymbol{\Phi}^-$. These are rectangular matrices of size $n \times s$ and the propagation constants $\boldsymbol{\Lambda}$ form a diagonal matrix of size s.

Bloch wave expansion can be used to estimate the nodal displacements in terms of this partial wave basis, as in Duhamel et al. (2006). For an infinite waveguide with waves propagating from a single location –the left interface of the cell number 0– we can estimate the left interface nodal displacements of k-th cell as:

$$\mathbf{q}_L^{[k]} \approx \boldsymbol{\Phi}^+\boldsymbol{\Lambda}^k\mathbf{a}^+ + \boldsymbol{\Phi}^-\boldsymbol{\Lambda}^{-k}\mathbf{a}^- \quad \forall k \in \mathbb{Z} \tag{3}$$

This approximation permits us to describe the waveguide dynamic motion in terms of the wave amplitudes $\mathbf{a}^+$, $\mathbf{a}^-$ that are related to physically meaningful waves –the Bloch modes–, i.e, torsional waves, compressional waves, flexural waves, etc. This approach is very common in the WFEM literature (Mead (2009); Mencik and Ichchou (2005)), because it avoids poor numerical conditioning of highly evanescent modes and better computational efficiency (Waki et al. (2009)).

3. WAVE SCATTERING THROUGH A COUPLING ELEMENT

The study of reflection and transmission of waves through a junction or coupling element in the WFEM framework started with the works of Mencik and Ichchou (2005); Ichchou et al. (2009). In these formulations, incident, reflected and transmitted waves are related among each other by means of nodal displacements and forces, and a *diffusion matrix* is obtained by linear least squares estimation (Moore-Penrose inverse). A first application of the method for wave-damage interaction was presented by Ichchou et al. (2009) and it required the use of Lagrange multipliers in the mortar method framework to perform a *mesh tying* and to ensure displacement field continuity between different mesh surfaces at the interface between the waveguide and the coupling element. Later Renno and Mace (2013) proposed a formulation for compatible meshes, i.e., without the need of Lagrange multipliers, but nodal displacements and force vectors were used and pseudoinversion remained as the solution of an overdeterminate system.

A practical formulation was presented in Droz et al. (2018) and later applied to damage detection in Droz et al. (2020). The Bloch wave expansion in an infinite waveguide expressed in (3) was used, altogether with a Bloch reduced order model (ROM), to describe the dynamic motion of a waveguide that encounters a junction or coupling element. Here, the formalism is presented in detail for the Bloch ROM. It is also shown that the formalism could be used in a standard WFEM framework, and this is applied in the next section to compare it against the Bloch ROM diffusion formulation.

Most wave modes evolve in the frequency domain with a certain smoothness, and this evolution can be described by a small collection of Bloch waves $\boldsymbol{\Phi}$ across the frequency range of interest selected after a singular value decomposition (SVD) to preserve the r relevant ones and form a Bloch wave basis $\boldsymbol{\Gamma}$ of size $n \times r$. This original idea was presented in Droz et al. (2014) for the study of coupled elasto-acoustic problems (e.g., fluid-filled pipes),

and it was improved in Boukadia et al. (2018). For the ROM projection, the $\mathbf{\Gamma}$ basis is combined with a component mode synthesis, namely Craig-Bampton reduction (Craig and Bampton (1968)). We have then the following projection matrix $\mathbf{B}$:

$$\mathbf{B} = \begin{bmatrix} \mathbf{\Gamma} & \mathbf{0} & \mathbf{0} \\ \mathbf{\Phi}_c^L \mathbf{\Gamma} & \mathbf{\Phi}_n & \mathbf{\Phi}_c^R \mathbf{\Gamma} \\ \mathbf{0} & \mathbf{0} & \mathbf{\Gamma} \end{bmatrix} \tag{4}$$

with $\mathbf{\Phi}_c^L$ and $\mathbf{\Phi}_c^R$ being the constrained modes, and $\mathbf{\Phi}_n$ being the dynamic modes. The relation between nodal displacements, forces and dynamic stiffness matrices of the full and reduced basis are projections, i.e., $\mathbf{q} = \mathbf{B}\tilde{\mathbf{q}}$, $\mathbf{f} = \mathbf{B}\tilde{\mathbf{f}}$ and $\tilde{\mathbb{D}} = \mathbf{B}^{\mathrm{H}}\mathbb{D}\mathbf{B}$.

The palindromic eigenproblem (2) can now be expressed with reduced dynamic stiffness matrices. Now the $2r$ eigenvalues λ are the propagation constants, and the $2r$ eigenvectors $\boldsymbol{\psi} \in \mathbb{C}^r$ are the reduced nodal displacements at a side boundary from which the Bloch waves can be recovered. Full solution of the eigenvalue problem gives us a similar set like in the partial Bloch basis $(\mathbf{\Phi}^+, \mathbf{\Phi}^-)$, but now $\mathbf{\Lambda}$ is a diagonal matrix of size r and $\mathbf{\Psi}^+$ and $\mathbf{\Psi}^-$ are square matrices of size r. Moreover, the reduced nodal displacements can be approximated by the Bloch wave expansion as in (3).

The great advantage of this Bloch model order reduction is, firstly, that $r < s < n$ and for large models $r \ll n$, and secondly, $\mathbf{\Phi}^+$ and $\mathbf{\Phi}^-$ are square matrices of size r, which facilitates the formulation of boundary value problems, leading to determinate problems to find the wave amplitudes of the Bloch modes.

For the wave scattering problem, the FE model of the coupling element must respect the periodicity both in the geometry of the cross section and in the interface degrees of freedom to ensure continuity of the displacement field. Modeling the coupling element dynamic stiffness matrix $\mathbb{S}$, and recalling the ROM projection, we have $\tilde{\mathbb{S}} = \mathbf{B}^{\mathrm{H}}\mathbb{S}\mathbf{B}$, where this time the $\mathbf{B}$ matrix is obtained from the previously computed $\mathbf{\Gamma}$ matrix of the waveguide and the $\mathbf{\Phi}_c^L$, $\mathbf{\Phi}_c^R$, $\mathbf{\Phi}_n$ matrices from Craig-Bampton reduction on the coupling element.

For right-going waves, we have the wave amplitudes $\mathbf{a}^+$ of incident Bloch waves that get reflected in $\mathbf{a}^-$ and transmitted in $\mathbf{b}^+$ wave amplitudes, as depicted in Figure 2:

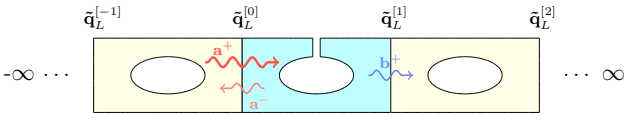

Fig. 2. Right-going waves on an infinite waveguide

The nodal displacements at the interfaces can be written:

$$\begin{cases} \forall k \in \mathbb{Z} \wedge k \leq 0: & \tilde{\mathbf{q}}_L^{[k]} = \mathbf{\Psi}^+ \mathbf{\Lambda}^k \mathbf{a}^+ + \mathbf{\Psi}^- \mathbf{\Lambda}^{-k} \mathbf{a}^- \\ \forall k \in \mathbb{Z} \wedge k \geq 1: & \tilde{\mathbf{q}}_L^{[k]} = \mathbf{\Psi}^+ \mathbf{\Lambda}^{k-1} \mathbf{b}^+ \\ \mathbf{a}^- = \mathbf{R}_{11}\mathbf{a}^+ & \\ \mathbf{b}^+ = \mathbf{T}_{21}\mathbf{a}^+ & \end{cases} \tag{5}$$

Recalling (1) and the internal equilibrium at the interfaces that gave us (2), we can write for both interfaces of the coupling element:

$$\begin{cases} \tilde{\mathbf{D}}_{RL}\tilde{\mathbf{q}}_L^{[-1]} + (\tilde{\mathbf{D}}_{RR} + \tilde{\mathbf{S}}_{LL})\tilde{\mathbf{q}}_L^{[0]} + \tilde{\mathbf{S}}_{LR}\tilde{\mathbf{q}}_L^{[1]} = \mathbf{0} \\ \tilde{\mathbf{S}}_{RL}\tilde{\mathbf{q}}_L^{[0]} + (\tilde{\mathbf{S}}_{RR} + \tilde{\mathbf{D}}_{LL})\tilde{\mathbf{q}}_L^{[1]} + \tilde{\mathbf{D}}_{LR}\tilde{\mathbf{q}}_L^{[2]} = \mathbf{0} \end{cases} \tag{6}$$

With (5) in (6) we can compute the reflection and transmission matrices $\mathbf{R}_{11}$ and $\mathbf{T}_{21}$, considering the *scattering matrix* $\mathbf{A}$:

$$\begin{cases} \mathbf{A}_{11} = \tilde{\mathbf{D}}_{RL}\mathbf{\Psi}^-\mathbf{\Lambda} + (\tilde{\mathbf{D}}_{RR} + \tilde{\mathbf{S}}_{LL})\mathbf{\Psi}^- \\ \mathbf{A}_{12} = \tilde{\mathbf{S}}_{LR}\mathbf{\Psi}^+ \\ \mathbf{A}_{21} = \tilde{\mathbf{S}}_{RL}\mathbf{\Psi}^- \\ \mathbf{A}_{22} = (\tilde{\mathbf{S}}_{RR} + \tilde{\mathbf{D}}_{LL})\mathbf{\Psi}^+ + \tilde{\mathbf{D}}_{LR}\mathbf{\Psi}^+\mathbf{\Lambda} \end{cases}$$

and by solving our determinate system, we obtain:

$$\begin{bmatrix} \mathbf{R}_{11} \\ \mathbf{T}_{21} \end{bmatrix} = -\mathbf{A}^{-1} \begin{bmatrix} \tilde{\mathbf{D}}_{RL}\mathbf{\Psi}^+\mathbf{\Lambda}^{-1} + (\tilde{\mathbf{D}}_{RR} + \tilde{\mathbf{S}}_{LL})\mathbf{\Psi}^+ \\ \tilde{\mathbf{S}}_{RL}\mathbf{\Psi}^+ \end{bmatrix} \tag{7}$$

In like manner, for left-going waves we have the wave amplitudes $\mathbf{b}^-$ of incident Bloch waves that get reflected in $\mathbf{b}^+$ and transmitted in $\mathbf{a}^-$ wave amplitudes, as depicted in Figure 3:

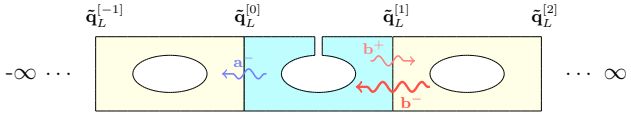

Fig. 3. Left-going waves on an infinite waveguide

Writing the nodal displacements as:

$$\begin{cases} \forall k \in \mathbb{Z} \wedge k \leq 0: & \tilde{\mathbf{q}}_L^{[k]} = \mathbf{\Psi}^- \mathbf{\Lambda}^{-k} \mathbf{a}^- \\ \forall k \in \mathbb{Z} \wedge k \geq 1: & \tilde{\mathbf{q}}_L^{[k]} = \mathbf{\Psi}^+ \mathbf{\Lambda}^{k-1} \mathbf{b}^+ + \mathbf{\Psi}^- \mathbf{\Lambda}^{-(k-1)} \mathbf{b}^- \\ \mathbf{b}^+ = \mathbf{R}_{22}\mathbf{b}^- & \\ \mathbf{a}^- = \mathbf{T}_{12}\mathbf{b}^- & \end{cases} \tag{8}$$

we obtain the reflection and transmission matrices $\mathbf{R}_{22}$ and $\mathbf{T}_{12}$ as:

$$\begin{bmatrix} \mathbf{T}_{12} \\ \mathbf{R}_{22} \end{bmatrix} = -\mathbf{A}^{-1} \begin{bmatrix} \tilde{\mathbf{S}}_{LR}\mathbf{\Psi}^- \\ \tilde{\mathbf{D}}_{LR}\mathbf{\Psi}^-\mathbf{\Lambda}^{-1} + (\tilde{\mathbf{S}}_{RR} + \tilde{\mathbf{D}}_{LL})\mathbf{\Psi}^- \end{bmatrix} \tag{9}$$

Although the formalism presented here concerns the Bloch ROM, the diffusion relations (7) and (9) can be developed for a Bloch basis with non-reduced dynamic stiffness matrices in (6), which implies that the $\mathbf{\Psi}$ matrices will be replaced by the $\mathbf{\Phi}$ matrices. It is important to note that

the size of the scattering matrix $\mathbf{A}$ is not anymore $2r \times 2r$ but $2n \times 2r$, giving an overdeterminate system. This will be referred as the standard WFEM or Bloch basis $\mathbf{\Phi}$ in the next section, since no Bloch wave-based ROM is applied.

4. NUMERICAL APPLICATION

As an application of the previous methodology, we present a diffusion analysis in a finned tube heat exchanger. This kind of structures is likely to be inspected by guided waves for damage detection (Malinowski et al. (2015)) and results of its numerical modeling such as the dispersion curves help in the selection of wave modes and frequency ranges before *in situ* testing. Moreover, damage models can be generated to understand how the propagating waves in the waveguide interact with them, therefore, diffusion curves help select wave modes sensitive to certain kinds of damage in a defined frequency range. Another important application of the diffusion analysis is the time domain reconstruction of a wave scattering through damage problem by means of Fourier synthesis. This is included in commercial softwares for guided wave based nondestructive evaluation, as explained in Baronian et al. (2016).

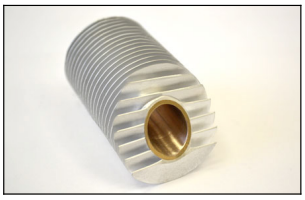

Fig. 4. Industrial finned tube heat exchanger. Credit: Thermofin.

The numerical model of the heat-exchanger unit cell and the coupling element –which aims to reproduce a corrosion-induced section loss– are shown in Figure 5. Unit cell and coupling element sizes are $d = 6.35$ mm, and their left and right interfaces have the same mesh, with $n = 1140$ DOF. The heat-exchanger materials are aluminum (fins) and copper (inner tube).

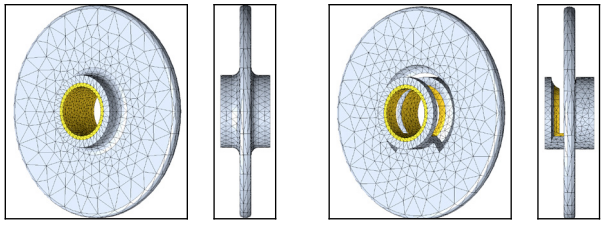

Fig. 5. The unit cell of the heat exchanger (left) and the coupling element as a section loss (right).

Dispersion curves of the unit cell are shown in Figure 6, they show the real part of the wavenumber $\Re(k)$, which are solutions of the reduced palindromic eigenproblem over the frequency range [0, 20] kHz. We can identify six propagating modes, and we can note that the compressional mode goes evanescent around 14 kHz, flexural modes undergo a conversion around 13 kHz (two wave modes are needed to represent a flexural mode in an axisymmetric structure). In contrast, torsional mode remains a propagating one through the whole frequency range.

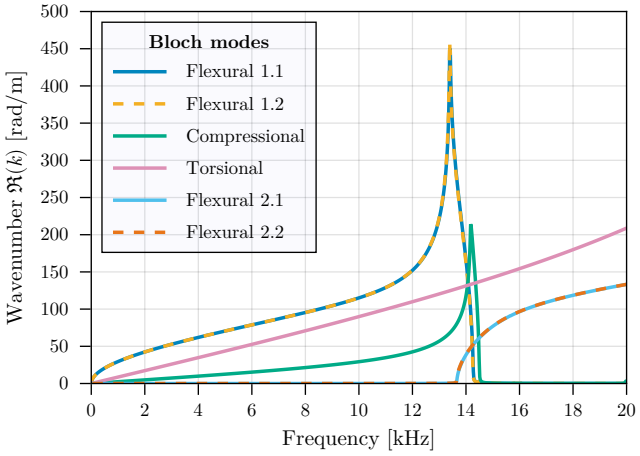

Fig. 6. Dispersion curves of the heat-exchanger unit cell.

Diffusion curves that represent wave scattering through the coupling element are shown in Figure 7, they show, for a mode j, the reflection ($R^2 = \mathbf{R}_{11}{}^2_{jj}$), transmission ($T^2 = \mathbf{T}_{21}{}^2_{jj}$) and diffusion ($\delta = 1 - R^2 - T^2$) amplitudes through the frequency range [0, 10] kHz, to remain in a zone without mode conversion in the waveguide. We can see that the presence of the damage does not significantly alter a compressional wave. In contrast, the torsional wave gets significantly reflected with almost no transmission in the frequency ranges [1, 3] kHz and [5, 10] kHz. These results encourage the selection of a torsional wave in the range [5, 10] kHz for this particular damage detection.

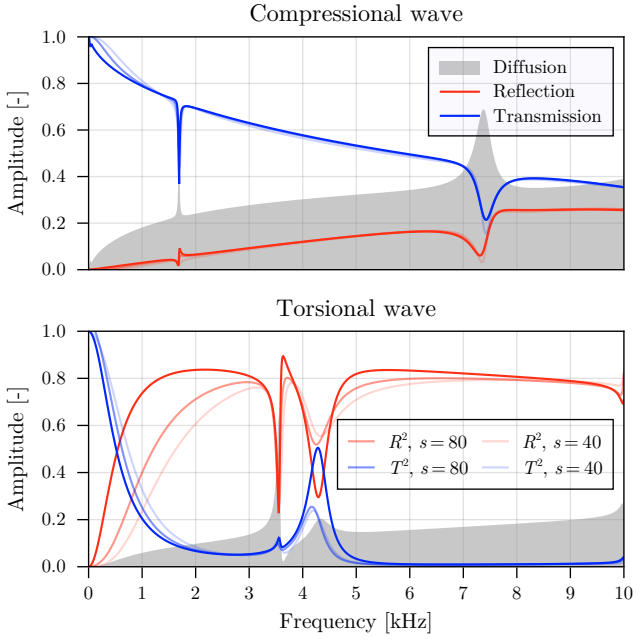

Fig. 7. Diffusion curves for compressional (above) and torsional (below) wave modes.

A relevant method comparison is also shown in Figure 7, since reflection, transmission and diffusion curves are shown for the Bloch ROM, but also reflection and transmission curves with lower opacity are shown for the Bloch

basis $\mathbf{\Phi}$ model, aiming to show that results appear to converge towards the ROM solution when increasing the number of waves s in the Bloch basis, but also computation costs are significantly higher, as shown in Table 1. Additional computation times of this numerical application are the Craig-Bampton reduction of the waveguide unit cell (1 m 50 s), the Craig-Bampton reduction of the coupling element (29 s) and the Bloch ROM (1 m 02 s).

Table 1. Method comparison

Method	Size	Time	ROM Factor
Bloch ROM - $\mathbf{\Psi}$	$r = 40$	17 s	1
Bloch basis - $\mathbf{\Phi}$	$n = 1140$, $s = 40$	36 m 22 s	128
Bloch basis - $\mathbf{\Phi}$	$n = 1140$, $s = 80$	58 m 08 s	205

Using Bloch basis $\mathbf{\Phi}$ can be at least 128 times more expensive than the Bloch ROM $\mathbf{\Psi}$, when setting $s = r$ to compare both methods with the same number of waves. Nonetheless, $s = r$ does not show good agreement with the Bloch ROM results, and so $s = 2r$ was tried, showing that diffusion results tend to fit the ROM results, but at a higher cost (205 times the ROM cost).

5. CONCLUSION

Numerical simulations are helpful to properly understand wave propagation and its interactions with damages to extend the guided wave testing practice to the nondestructive evaluation of periodic structures. In the WFEM context, diffusion analyses involve an overdeterminate system, solved through linear least squares estimation. A Bloch wave-based model order reduction was included into the diffusion analysis, which gives us the benefit of a smaller determinate problem, i.e., less computation time and higher accuracy.

Beyond increased accuracy and faster convergence, the number of Bloch waves r can be significantly smaller than the number of interface degrees of freedom n, which reduces the cost of the partial eigenvalue problem solved at each frequency. For the presented model, with $r = 40$ and $n = 1140$, reduction factors as high as 205 were found when compared against a standard WFEM formulation. These results strongly encourage the exploration of massively generated wave-damage scenarios through machine learning techniques to perform model-assisted guided wave testing in periodic waveguides.

REFERENCES

Baronian, V., Jezzine, K., et al. (2016). Simulation of NDT inspection in 3D elastic waveguide involving arbitrary defect. In *19th world conference on non-destructive testing, Munich*, 13–17.

Boukadia, R.F., Droz, C., Ichchou, M.N., and Desmet, W. (2018). A Bloch wave reduction scheme for ultrafast band diagram and dynamic response computation in periodic structures. *Finite Elements in Analysis and Design*, 148.

Cawley, P. (2018). Structural health monitoring: Closing the gap between research and industrial deployment. *Structural Health Monitoring*, 17(5), 1225–1244.

Craig, R.R. and Bampton, M.C.C. (1968). Coupling of substructures for dynamic analyses. *AIAA Journal*, 6(7), 1313–1319.

Droz, C., Lainé, J.P., Ichchou, M.N., and Inquiété, G. (2014). A reduced formulation for the free-wave propagation analysis in composite structures. *Composite Structures*, 113, 134–144.

Droz, C., Boukadia, R., Deckers, E., and Desmet, W. (2020). Sub-wavelength damage detectability assessement in periodic assemblies using a Bloch modelling framework. In *Proceedings of the XI Internationa Conference on Structural Dynamics, EURODYN2020*, 870–877.

Droz, C., Boukadia, R., Ichchou, M., and Desmet, W. (2018). Diffusion-based design of locally resonant subsystems using a reduced wave finite element framework. In *Proceedings of ISMA2018 and USD2018*.

Duhamel, D., Mace, B., and Brennan, M. (2006). Finite element analysis of the vibrations of waveguides and periodic structures. *Journal of Sound and Vibration*, 294(1), 205–220.

Fiborek, P. and Kudela, P. (2021). Model-Assisted Guided-Wave-Based Approach for Disbond Detection and Size Estimation in Honeycomb Sandwich Composites. *Sensors*, 21(24).

Huang, T.M., Lin, W.W., and Qian, J. (2009). Structure-preserving algorithms for palindromic quadratic eigenvalue problems arising from vibration of fast trains. *SIAM Journal on Matrix Analysis and Applications*, 30(4), 1566–1592.

Ichchou, M., Mencik, J.M., and Zhou, W. (2009). Wave finite elements for low and mid-frequency description of coupled structures with damage. *Computer Methods in Applied Mechanics and Engineering*, 198(15), 1311–1326.

Malinowski, O.M., Lindsey, M.S., and Van Velsor, J.K. (2015). *Ultrasonic Guided Wave Testing of Finned Tubing*. Pressure Vessels and Piping Conference. ASME.

Mead, D.J. (1973). A general theory of harmonic wave propagation in linear periodic systems with multiple coupling. *Journal of Sound and Vibration*, 27(2), 235–260.

Mead, D.J. (2009). The forced vibration of one-dimensional multi-coupled periodic structures: An application to finite element analysis. *Journal of Sound and Vibration*, 319(1), 282–304.

Mencik, J.M. and Ichchou, M. (2005). Multi-mode propagation and diffusion in structures through finite elements. *European Journal of Mechanics - A/Solids*, 24(5), 877–898.

Renno, J.M. and Mace, B.R. (2013). Calculation of reflection and transmission coefficients of joints using a hybrid finite element/wave and finite element approach. *Journal of Sound and Vibration*, 332(9), 2149–2164.

Ricci, F., Monaco, E., Boffa, N., Maio, L., and Memmolo, V. (2022). Guided waves for structural health monitoring in composites: A review and implementation strategies. *Progress in Aerospace Sciences*, 129, 100790.

Waki, Y., Mace, B., and Brennan, M. (2009). Numerical issues concerning the wave and finite element method for free and forced vibrations of waveguides. *Journal of Sound and Vibration*, 327(1), 92–108.

Willberg, C., Duczek, S., Vivar-Perez, J.M., and Ahmad, Z.A.B. (2015). Simulation Methods for Guided Wave-Based Structural Health Monitoring: A Review. *Applied Mechanics Reviews*, 67(1), 010803.